Using neutron activation analysis to identify scales of interaction at Kinet Höyük, Turkey

Peter Grave [a,*], Lisa Kealhofer [b], Ben Marsh [c], Marie-Henriette Gates [d]

[a] *Department of Archaeology and Palaeoanthropology, University of New England, Armidale, NSW 2351, Australia*
[b] *Anthropology/Environmental Studies Institute, Santa Clara University, Santa Clara, CA 95050, USA*
[c] *Department of Geography and Environmental Studies, Bucknell University, Lewisburg, PA 17837, USA*
[d] *Department of Archaeology and History of Art, Bilkent University, Ankara 06800, Turkey*

Abstract

We use NAA to characterize a relatively large archaeological ceramic sample from the Late Bronze Age to Hellenistic phases of Kinet Höyük, a coastal Turkish site in the Gulf of Iskenderun at the northeast corner of the Mediterranean Sea. The geographic extent of local Kinet wares (how local is local?) is established through comparison with sediment samples across the Kinet hinterland. Four major compositional groups are identified: local and locally imported wares, imports from Cypriot, and presumed Western Anatolian and Aegean centers, and imports that appear relatively homogenous elementally but comprise typologically diverse ceramics with attributions that range from Cyprus to the coastal mainland. Comparison with other published NAA studies for this site reinforces the elemental evidence for local production, and underlines the need for caution when assuming local production always equates with local clays particularly for coastal sites. We propose that the chronological distribution of the local and non-local groups provides a useful political economic proxy. The study indicates systemic and widespread political disruption and marginalization at the transition to the Late Iron Age in this region.
© 2008 Elsevier Ltd. All rights reserved.

Keywords: Mediterranean trade; Political dynamics; Iron Age; Multivariate analysis; Local production

1. Introduction

Archaeologists have long debated the social and economic changes that occurred during the transition from the Late Bronze Age (LBA) to the Iron Age (IA) in the eastern Mediterranean (Carpenter, 1966; Sherratt, 1993a,b; Sherratt and Sherratt, 1993). The widespread political collapse of Mycenaean, Ramesside Egyptian, and Hittite empires at the end of the LBA and the emergence of new maritime trade networks are the backdrop for the formation of new political economies in the IA. In this paper, we present and discuss Neutron Activation Analysis (NAA) characterization of LBA, IA and Hellenistic ceramics from the site of Kinet Höyük, in the northeastern Mediterranean, as part of a wider project to evaluate the nature of political economic change during this volatile period in western and central Anatolia (The Anatolian Iron Age Ceramics Project: http://aia.une.edu.au).

The present study has two broad aims: one substantive, the other methodological. In order to evaluate the potential of using Kinet ceramics (production and exchange) as a proxy for regional political dynamics, we first aim to establish the structure and range of elemental signatures for local, regional and imported ceramics. Achieving this goal not only requires a large sample for analysis, appropriate analytic instrumentation and data handling techniques, but also involves differentiation of a comparatively large number of compositional groups whose membership can be ambiguous. Two previous NAA studies at Kinet provide the potential to further expand the analytic database for this site and we evaluate the extent to which these datasets, from different facilities, can be integrated into the present work.

* Corresponding author. Tel.: +61 2 6773 2062; fax: +61 2 6773 3030.
  E-mail address: pgrave@une.edu.au (P. Grave).

2. Background

2.1. Ceramics as proxies of political dynamics

Traditionally, archaeologists have used settlement patterns to describe the scale and nature of polities (Adams, 1981; Adams and Nissen, 1972; Blanton, 2004; Magee, 2004). Settlement size, location and phasing are used to reconstruct the organization and population density of regions over time, while artifacts like ceramics often form the basis of the chronology and the stylistic/cultural links between contemporary settlements.

In this study, we use the pattern of local, regional, and exotic ceramic production and exchange as a proxy for the political economic position of a site—in this case Kinet Höyük—and its region. We suggest that differences in the relative amount of local vs. regional vs. imported ceramics, when seriated through a site's history, contribute an important line of evidence for understanding the larger regional pattern of political and economic change. NAA analysis of ceramics from Megiddo was used to suggest that this type of data, for a relatively small but diverse assemblage ($n = 86$), can provide insight into the political dynamics of the southern Levant in the EIA (Harrison and Hancock, 2005). More recently, a NAA study of Maya ceramics at Teotihuacan was used to make comparable arguments for the linkages between ceramic exchange and political economies (Clayton, 2006).

Kinet Höyük is a small but steep mound (3.3 ha, 26 m high) situated between a shallow bay and the north bank of an estuary. These two harbors provided port facilities and the site's main economic resource throughout much of its settlement history, from the Late Neolithic to the end of the Hellenistic period (ca. 5300–50 B.C.). Kinet was refounded briefly as a medieval commercial center and border post during the 12th to 14th centuries A.D., by which time the estuary had silted in

and the river flowed several km to the south. Excavations conducted from 1992 to 2007 indicate that the Bronze Age town extended beyond the mound to include a low-lying district along the north shoreline, and was at least twice the size of today's visible ancient topographic features. The lower town and its citadel continued to be occupied through the end of the MIA. With the LIA, however, settlement contracted to the mound proper, and maintained this limited scale during the Hellenistic and medieval periods.

The location of Kinet Höyük (Fig. 1), in a region long identified as a crossroads between East and West trade (the maritime Mediterranean and overland Mesopotamian trade routes), as well as between the Levant and central Anatolia, is critically placed for understanding how regional polities responded to the collapse of the Hittite empire and the formation of more fluid Iron Age maritime economies (Polanyi, 1963; Woolley, 1946). Ceramic stylistic typologies have been very influential in this region for establishing the timing of a transition from Cypriot to Aegean/Greek trade networks during the Iron Age (Boardman, 1965; Lehmann, 1998; Lehmann, 2005). However, a weakness of these characterizations is the conflation of ceramic typologies from well recognized as well as presumed origins. We use a compositional approach to determine local, regional and long-distance patterns of production and exchange and the nature of local political dynamics in this region, independent of typological criteria or assumed origins.

2.2. Methodological issues

The scale of an analytic study can rarely match that of an archaeological assemblage (Rhode, 1988). In sampling ceramics a common research strategy is to concentrate on a single or a few types of a particular period to distinguish, for example,
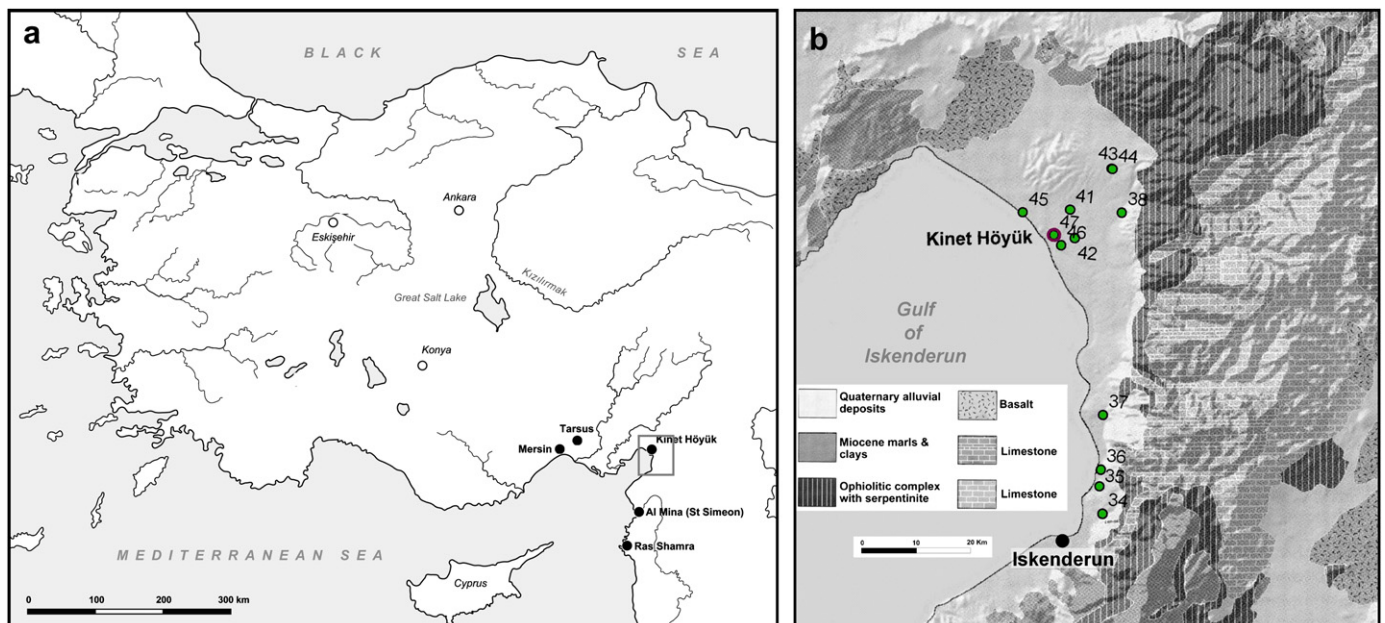

Fig. 1. (a) Map of Turkey showing location of Kinet Höyük and some principal sites mentioned in the text. (b) Composite map of geology and elevation for Kinet Höyük and hinterland with locations of sediment samples discussed in text and presented in Tables 2A and B (adapted from Hodos et al., 2005, figure 4).

imports from emulations (Liddy, 1988). In this top-down approach, identification of a production center relies on reference samples of known origin (Harbottle et al., 2005; King et al., 1986), or less reliably, find spot frequencies based on the abundance of a particular type in a regional assemblage (Brodie and Steel, 1996; Knappett et al., 2005). A typology driven, top-down analytic strategy effectively tests group membership within a pre-determined range. However, it is notably deficient where groups are not well defined or where a goal is to identify new or unanticipated groups (Dibble, 1988). To develop a political proxy from analyses of a functionally, typologically, and chronologically diverse ceramic assemblage requires a sampling strategy that enables a representative selection of the range of local, regional and exotic wares. By sampling the full range of local/regional/exotic wares over time, we aim to better define how political economic dynamics shift throughout a site's occupation. To achieve this we adopt an assemblage driven, bottom-up sampling strategy.

An important step in determining different production areas is to define artifact provenance. The use of "compositional profiles of artefacts and source materials to trace individual artefacts from their find spot to their place of origin" (Glascock and Neff, 2003), remains contingent on how well the geographic extent and geochemical context of a source is known (Neff, 2000). Where archaeological materials are derived from discrete geological sources (e.g. lithics from an obsidian source), the "provenance postulate" has proven highly effective (Ericson and Glascock, 2004; Glascock, 2002; Summerhayes et al., 1998; Tykot, 2002; Wilson and Pollard, 2001). But for ceramic provenance studies the definition of the geographic extent and geological context of clay beds used in antiquity remains a major challenge (Dorais et al., 2004; Schwedt and Mommsen, 2004). To identify local production at Kinet, we adopt a sampling strategy that targets sediments representing the geochemical range and diversity of the site catchment. These are used to bracket ceramic compositions of likely local origin.

3. Methods

3.1. Sampling strategy

Notwithstanding proposed strategies to counter sampling biases of a large and diverse archaeological assemblage (Baxter, 2001a), inherent skewing introduced both by patterns of discard and through excavation strategies makes any sampling strategy highly subjective. We seek to minimize sampling distortions through the expertise of the site ceramicist. For the present study, care was taken to try to ensure that sampling approximated the diversity of wares present in each phase.

3.2. Neutron activation analysis (NAA)

We employ NAA as the technique of choice for routine measurement of ceramic geochemistry. The analytical strengths of NAA for archaeological work have been detailed elsewhere (Bishop and Blackman, 2002; Glascock, 1992; Glascock

et al., 2004; Harbottle, 1982). The technique is capable of high sensitivity and precision for a wide suite of elements, is the reference method for several elements, and offers long term measurement stability (years or even decades). Because sample matrix effects are inconsequential, ceramic preparation requirements for NAA are minimal. In contrast, ceramic analysis with comparable, or more sensitive, elemental and isotopic measurement techniques (e.g. XRF, ICP-OES, ICP-MS, TIMS), involve a range of elaborate and exacting preparation methods (e.g. acid digestion, glass fusion, powder pelletization). These methods can not only present a major bottleneck for sample throughput, but can also introduce a host of method- and operator-specific idiosyncrasies that undermine both long term measurement stability and inter-facility comparisons.

Our NAA sample preparation involves removal of all surfaces of the sample with a tungsten carbide burr, followed by soaking for 72 h in distilled water to remove environmentally mobile salts, and oven-drying (Unruh and Johnson, 2005). On cooling, samples are wrapped in a disposable polyvinyl acetate sheet and crushed between steel plates using a manual hydraulic press. The crushed sample is submitted for analysis in a plastic vial labeled with a unique identifier linked to a descriptive database. For sediments, preparation involves screening in the field to remove larger (>3 mm) rock fractions, prior to submission for analysis.

Comparatively large, 1 g samples are submitted for irradiation and measurement. The averaging effect of large sample size is especially useful to compare results from fine and coarse or heterogeneous fabrics and sediments derived from the same source. Of the 33 elements routinely measured, 25 are retained that have good counting statistics based on comparison of results for standard reference materials (NIST 679, 2711, 1633B: Table 1).

3.3. Data analysis

Powerful analytic techniques for data patterning and group membership verification are needed to handle large data sets (Baxter, 1994, 2006). There is now broad agreement for the application of complementary multivariate techniques to identify compositional groups (i.e. Principal Components Analysis (PCA) for initial identification of compositional groups coupled with discriminant function analysis—Canonical Variates Analysis (CVA)—for verification) (Baxter, 2001b; Beier and Mommsen, 1994b; Harbottle, 1991). In top-down studies, a high degree of typological control is used to generate initial classification criteria for more precise comparison of known and unknown compositions and for group verification (Jones, 1986). Some consider that natural variations, especially in the amounts of quartz present, can significantly extend the apparent compositional range of a source ("dilution"), and will generate correction factors to improve group statistics (Beier and Mommsen, 1994a; Mommsen et al., 1988). Others use homogeneity as a measure of a compositional group and seek to minimize the coefficient of elemental variation (CV) (Blackman et al., 1993). These independent solutions to the problem of compositional group identification not only share

Table 1
NAA results for three standard reference materials (SRM 697, 2711 and 1633b) supplied by the National Institute for Standards and Technology, Washington, DC

ppm	SRM 2711 (n = 5)				SRM 679 (n = 5)				SRM 1633b (n = 5)			
	Avg.	CV	Cert/pub	% Recovery	Avg.	CV	Cert/pub	% Recovery	Avg.	CV	Cert/pub	% Recovery
As	101.7	3.14	–	–	9.64	9.19	–	–	130	1.96	136.2	95.45
Ba	794.2	18.1	726	109.39	465	12.72	432.2	107.59	687.5	10.58	709	96.97
Br	5.19	11.46	5	103.80	2.07	26.65	–	–	2.72	56.2	2.9	93.79
Ca%	3.3	6.1	2.88	114.58	–	–	0.16	–	2.23	5.2	1.51	147.90
Ce	72.78	3.79	69	105.48	103	3.29	105	98.10	184.8	2.95	190	97.26
Co	10.06	4.48	10	100.60	26.38	4.07	26	101.46	49.52	3.12	50	99.04
Cr	47	8.36	47	100.00	107.4	4.49	109.7	97.90	203.4	3.61	198.2	102.62
Cs	6.38	3.33	6.1	104.59	9.44	4.49	9.6	98.33	10.32	3.64	11	93.82
Eu	1.14	5.2	1.1	103.64	1.77	4.55	1.9	93.16	3.9	4.75	4.1	95.12
Fe%	2.86	2.95	2.89	98.96	8.75	3.48	9.05	96.69	7.58	2.54	7.78	97.43
Hf	8.28	3.72	7.3	113.42	4.49	4.86	4.6	97.61	6.64	5.52	6.8	97.65
K%	2.53	12.78	2.45	103.27	2.21	11.58	2.433	90.83	1.29	62.37	1.95	66.15
La	38.54	1.82	40	96.35	51.72	3.57	–	–	90.82	3.1	94	96.62
Lu	0.5	11.32	–	–	0.54	10.15	–	–	1.1	3.37	1.2	91.67
Na%	1.13	3.69	1.14	99.12	0.15	11.63	0.1304	115.03	0.22	7.93	0.201	109.45
Nd	29.86	5.87	31	96.32	42.62	6.05	–	–	82.92	4.05	85	97.55
Rb	110.94	9.16	110	100.85	184	4.91	190	96.84	137.8	10.11	140	98.43
Sb	19.28	2.97	–	–	0.92	25.14	–	–	5.13	4.41	6	85.50
Sc	9.47	4.36	9	105.22	22.76	3.38	22.5	101.16	40.8	2.66	41	99.51
Sm	6.12	1.7	5.9	103.73	8.96	2.6	–	–	18.1	1	20	90.50
Ta	1.29	4.49	2.47	52.23	1.09	7.22	–	–	1.73	6.78	1.8	96.11
Tb	0.76	14.61	–	–	0.94	57.09	–	–	2.56	15.77	2.6	98.46
Th	13.54	3.56	14	96.71	13.66	3.53	14	97.57	24.9	3.56	25.7	96.89
U	3.34	13.57	2.6	128.46	2.73	13.82	–	–	9.35	5.6	8.79	106.37
Yb	3.05	7.35	2.7	112.96	3.55	5.24	–	–	7.35	4.15	7.6	96.71
Zn	338.6	3.51	350.4	96.63	104.2	8.88	150	69.47	175.8	3.85	210	83.71

The table shows experimental results for five replicates measured during the analysis of the Kinet ceramic sample presented in this paper. Results are given as mean values with % coefficient of variation (CV) alongside certified/published values for each element and the deviation of the experimental mean from the certified/published values (% recovery). Elements reported as parts per million (ppm) unless otherwise indicated; "–" indicates below detectable limits.

a dependence on typology but also an assumption that group integrity should be synonymous with compositional homogeneity. Dilution corrections may mask real compositional differences between typologically similar types, and low CVs are not always a good measure of group integrity. Even for standards (cf. Table 1) higher CVs can result from detection limitations of already low level or difficult to measure elements (e.g. Tb, Ta, Cr, K%, Zn). For experimental results elemental variability can also reflect idiosyncrasies specific to a source, overall sample inhomogeneity, or incorporation of samples from marginally different but compositionally overlapping sources that cannot be differentiated. The classification procedures adopted here do not rely on assumptions of homogeneity but on point proximity and systematic gaps between point clusters in multivariate projections. This approach dispenses with *a priori* assumptions about compositional behavior and generally produces group statistics comparable to typology-driven, top down clustering methods.

A particular strength of PCA is that it can provide a graphic summary of compositional relationships, in particular, group compactness and group orientation. Compactness can be used as an indicator of the homogeneity or heterogeneity of a group fabric to differentiate, for example, different levels of processing for samples from the same source, or between samples from different catchments that have been derived from similar, relatively homogenous sources. Relative orientation of a group is driven by source-specific elemental correlations. Typically, for samples derived from catchments with different geologies, PCA projections show marked differences in relative group orientation.

To more fully exploit the potential of multivariate analysis to assist in group formation we use an analytic software package capable of dynamic three-dimensional classification (SAS Institute, 2006). In this approach, point scatter projections are interactively rotated on the first three components (for PCA) to understand the structural characteristics of compositional groups. Group membership, initially assigned during the PCA examination, is then checked with CVA, in a procedure where membership probability is evaluated using a multivariate distance criterion (sum of squares). The results are further cross-checked with contextual and typological information. Where a dataset is highly structured, this procedure typically identifies a relatively small number of compositional groups, each of which is composed of outer groups that are most compositionally distinct and within these, an inner core of more closely packed, compositionally similar groups. Finer compositional structure is identified through iterative "peeling away" of groups (i.e. as outer groups are identified they are removed and the remaining dataset is reanalyzed using the same PCA/CVA combination, with finer grained structure identified and further classified). The process is repeated until no further groups can be distinguished.

4. The sample

Two hundred and ninety ceramics and 12 geological sediments are used in this study. The ceramics span a period from the Late Bronze Age (LBA) to the Hellenistic period. The uneven spread of samples across periods (LBA strata 13.1–13.2 and IA 12-11-10 and 7 best represented) can be taken as a general reflection of the excavated phases at the site (Fig. 2).

Geological samples were collected from watersheds chosen to represent distinctive upland lithologies (Fig. 1b, Tables 2A, 2B). The primary local lithological differences are between various ophiolitic melange components, a range of neretic and pelagic limestones, and lacustrine marls and siltstones. Two main areas were identified for sampling: one leading into the ophiolite dominated watershed behind the site; the other at the south end of the coastal plain where there is greater intermingling of ophiolite and limestone bedrocks. Samples were collected from stream and slope deposits distinctive of particular rock types, and from sedimentary deposits with different amounts of transport and mixing. Samples of visually similar ophiolitic sediments were collected from multiple points along the mountain front behind the coastal plain, to identify geochemical variability. Samples of humanly transported earth materials were collected as brickwash from IA horizons of the mound, and as wasters from an abandoned modern tile works near the mound. Local reports about the raw material for the tile works suggest that it was brought from a regionally important clay bed of Miocene marls south of the city of Iskenderun, 28 km south of Kinet.

5. Results

The Anatolian Iron Age project adopts a site-specific nomenclature in labeling compositional groups. For Kinet Höyük groups are assigned the prefix KH. The Kinet NAA dataset is composed of four major compositional groups (KH1–KH4), with KH1 identified as the Kinet signature group based on sediment matches and the remaining groups as imported wares (Fig. 3a–d, Table 3). Overall, KH1 samples are dominated by very high chromium values. This general group is composed of three subsets of varying size and compactness. In the PCA projection, KH1.1 appears as the most distant and least compact, and within it is a smaller relatively compact group (KH1.2). The last group (KH1.3), close to the projection centroid, is marginally more compact than KH1.1. Typologically, a limited range of buff coarse fabrics and larger wares predominate in the KH1 groups. While decorated wares are rare, the majority belong to KH1.1. They include a local emulation of a Hittite style red burnished jug with straight spout (Period 15, LBI) as well as regionally typical Iron Age bichrome and monochrome painted vessels (Fig. 4a 1–4).

Sediment geochemistry is dominated by the ophiolitic geology of the coastal range in this region. However, the multivariate
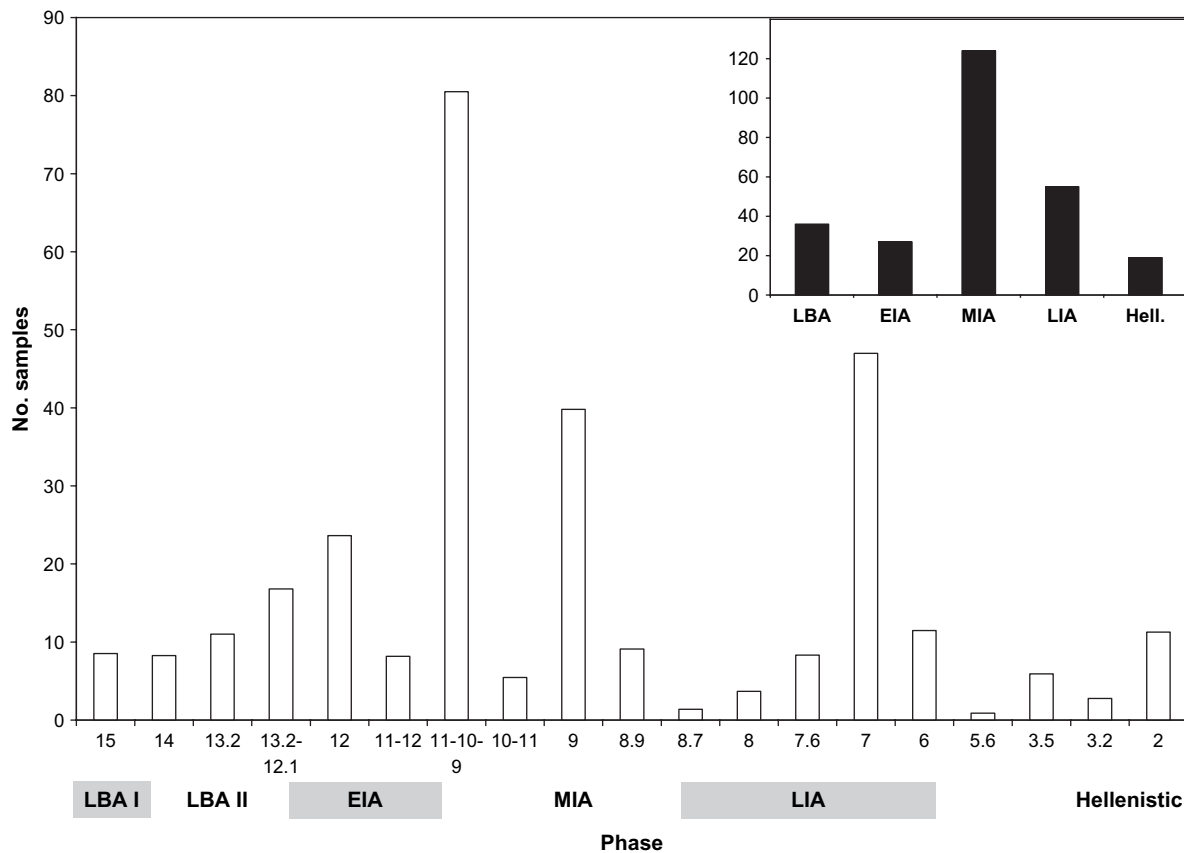

Fig. 2. Frequency histogram of chronological phases (from the site) represented in the Kinet ceramic sample, and (inset) summary of number of samples by chronological period (LBA = Late Bronze Age; EIA = Early Iron Age; MIA = Middle Iron Age; LIA = Late Iron Age).

Table 2A
Description and locations (UTM coordinates) for Kinet sediments used in this study

AIA #	Fig. 1b #	Group	UTM Reference			Description
			zone	easting	northing	
2252	38	KH1.1	37	253481	4084804	Steep fan at mountain face; ophiolite cobbles, red soil inter bedding 20 m down
2253	41	KH1.1	37	248474	4085203	1.5 m down-section in low gradient fan
2255	43	KH1.1	37	252578	4089096	Alluvial surface soil above 1st drainage N of Kinet; 0.5 m down section
2256	44	KH1.1	37	252656	4089043	Terra rosa on travertine, N drainage
2257	45	KH1.1	37	243898	4085035	Lagoon fill, 200 m inland, surface grab
2258	46	KH1.1	37	247536	4081762	Surface grab, soil overbank, middle stream pos., Deliçay
2259	47	KH1.1	37	246845	4082746	Kinet Höyük Phase 9 (late MIA); 8th c BC
2248	34	KH1.3	37	250979	4055637	Very rocky bank
2249	35	KH1.3	37	250743	4058279	6 m down big stream bank; v/ blocky
2251	37	KH1.3	37	251247	4065221	Fan deposits 2 m down road cut 15 ks. Dörtyol
2254	42	KH1.3	37	248877	4082451	Waster at tile works, Yeşilköy
2250	36	KH3	37	250908	4259925	Road cutting, limestone soil, 3 m down

spread of KH1.1 and KH1.3 also has a spatial corollary in the sediments. One set of sediments from the immediate environs of the site matches KH1.1/1.2 compositions, and a second set of sediments from the more southern sampling area matches KH1.3. The comparison establishes the local scale of the ceramics in the KH1.1 group and a probable more distant local origin for KH1.3. Included in the KH1.3 sediment group is the waster from the tile works at nearby Yeşilköy, thought to be made from clays near Iskenderun. The lack of sediment matches with the remaining three groups, KH2—KH4, strongly suggests they represent the non-local component of the sample.

The range of typologies present in the comparatively large and undifferentiated KH2 groups suggests diverse production centers but use of a widespread sediment type. The structural proximity to KH1.3 may indicate that KH2 sediments are derived from reworked coastal sediments similar to those of the Kinet environment but without the high chromium ophiolitic component. KH2 consists of two major core groups (KH2.1, KH2.2) and several smaller groups (Fig. 3b). Typologically, the two major groups contain a wide range of wares: buff, red and white slipped monochrome and bichrome, black on red wares (some identified as Cypriot, Fig. 4b 4,5), figural

(Cyprio-Archaic) Cypriot wares (Fig. 4b 2,3), Eastern Sigillata A (Fig. 4b 8—12) and other red slip fine wares. Less common are coarse undecorated bowls, cooking pots and amphoras assigned an origin in the Late Iron Age Levant (Fig. 4b 14). One of the outlying subsets (KH2.6) represents a second type of black on red banded bowl (Fig. 4b 15,16) discussed further below.

The numerous compositional divisions and relatively high typological diversity of KH3 are also consistent with multiple production centers using a wide range of geologically similar sources (Fig. 4c 1—13). For KH3, a distinctive pattern of elevated trace and rare earth elements that separates it from the other major groups also suggests that this group is derived from a different type of geology (Table 3). Structurally, KH3 is composed of two major groups (KH3A, KH3B) that spread out along different elemental trajectories. KH3B breaks down into a number of subgroups (Fig. 3c, Table 4). KH3A contains seven discrete, compositionally very similar, groups (Fig. 3d, Table 5). While close, these compositional groups are also typologically discrete (Ionian, East Greek, Samian, Euboean, or Rhodian centers). Other KH3A groups contain typologically well known trade wares of uncertain provenience. These

Table 2B
NAA results for Kinet sediments used in this study

| AIA #	Fig.1b #	Group	INAA																								
			As	Ba	Ca%	Ce	Co	Cr	Cs	Eu	Fe%	Hf	K%	La	Lu	Na%	Nd	Rb	Sb	Sc	Sm	Ta	Tb	Th	U	Yb	Zn
2252	38	KH1.1	1	75	1.5	11	125	3390	0.8	0.21	7.31	0.8	0.3	5.7	0.05	0.1	8	11	0.2	11.7	0.86	0	0.3	1.6	0	0.44	58
2253	41	KH1.1	21	74	5.4	25	81.7	1710	2.2	0.44	5.44	2	0.5	12.4	0.11	0.24	11	19	4.1	11	2.21	0	0.4	3.1	2	1	48
2255	43	KH1.1	27	62	2.5	23	104	2880	1.3	0.48	7.17	1.8	0.7	12.7	0.1	0.31	13	21	7.2	15	2.24	0.9	0.5	2.7	1	1	64
2256	44	KH1.1	22	75	1.7	45	86.2	2530	3.3	0.95	7.5	3.2	0.4	24.4	0.22	0.19	19	48	6.7	17	4.14	1.1	0.6	6.3	1.8	1.8	72
2257	45	KH1.1	18	85	2.4	26	88.1	3200	2.2	0.57	6.42	1.6	0.7	13.4	0.13	0.13	9	32	4.8	13.5	2.35	1	0.5	3.6	1.3	1	76
2258	46	KH1.1	6	120	1.1	24	93.7	1800	1.9	0.46	5.8	2	0.9	13	0.12	0.18	12	29	1.6	11.3	2.23	0.6	0	3.4	1.9	1	54
2259	47	KH1.1	7	110	6.3	20	62.1	1300	1.3	0.52	3.79	1.6	0.4	10.6	0.1	0.2	12	27	1.8	7.85	1.78	0.6	0.3	2.4	1.5	0.74	71
2248	34	KH1.3	2	0	14	4	55.5	2910	0.6	0.24	4.07	0.3	0	3.5	0.08	0.26	8	0	0.2	12.4	0.71	0	0	0.5	0	0.54	41
2249	35	KH1.3	7	88	18	10	63.3	3540	1.6	0.25	4.47	0.8	0.3	7	0.08	0.15	10	13	0.9	10.8	1.16	0	0	1.6	1	0.65	72
2251	37	KH1.3	15	71	14	22	56.7	1720	2.3	0.63	4.69	2	0.6	12	0.13	0.12	14	29	1.8	8.99	2.22	0.6	0	2.9	2.1	1	68
2254	42	KH1.3	17	140	10	35	48	785	6.5	1	5	2.3	1.1	19.3	0.24	0.75	17	54	1.6	17.3	3.5	0	0.7	6	6	1.9	140
2250	36	KH3	8	310	2.7	84	34	428	6.6	1.2	4.8	4.4	1	34.5	0.32	0.23	23	72	1.1	16.9	5.03	1	0.9	11	1.8	2.4	110
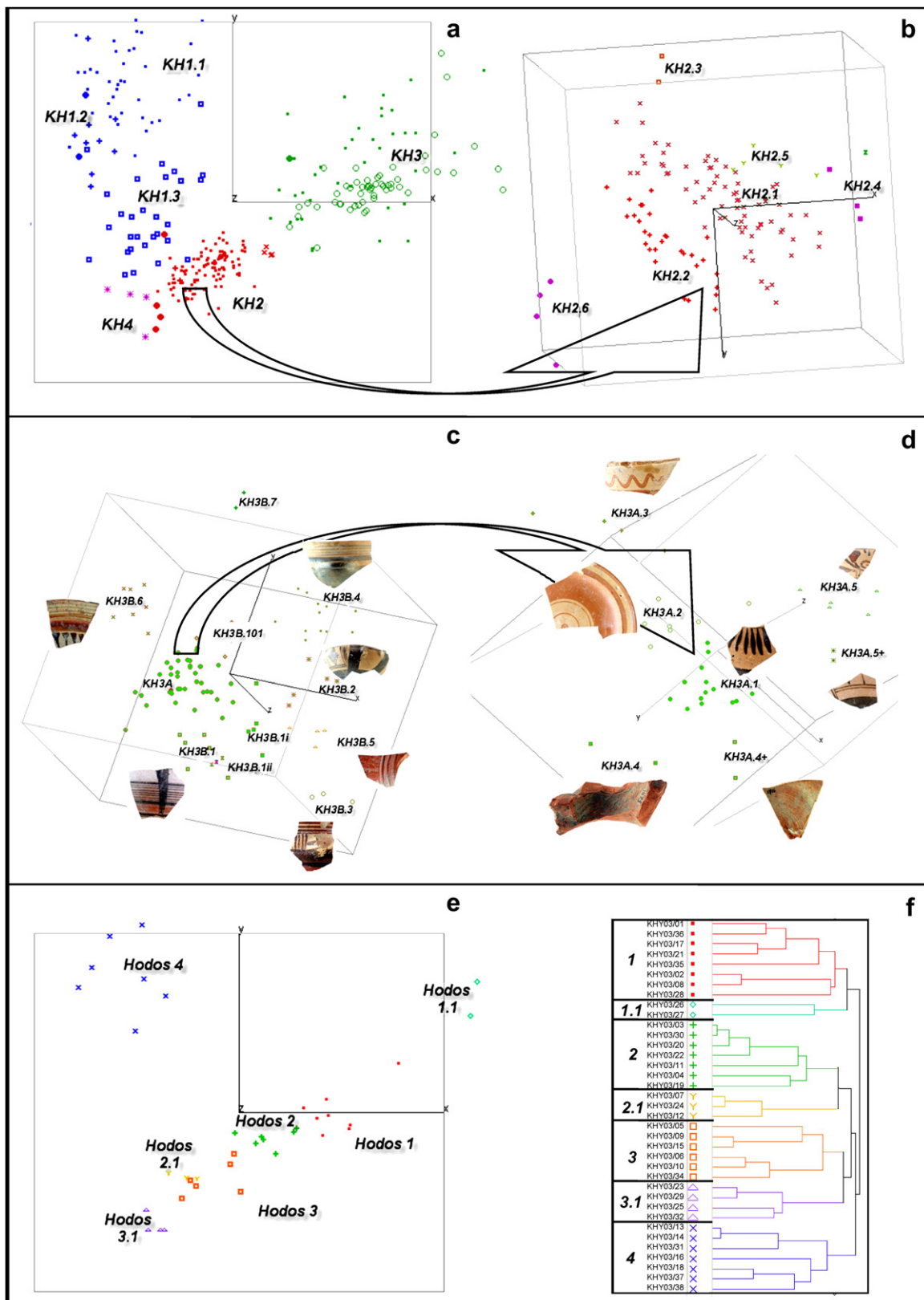
Fig. 3. Principal components analysis projection for the complete dataset with major groups and subsets labeled: (a) distribution of samples on the first two components (solid circles in the KH1 subsets indicate sediments); (b) Principal components analysis of the KH2 group. Rotated projection on the first three components showing distinction between main subsets (KH2.1 and 2.1) and the relative position of outlying subsets (KH2.3−2.6; note KH2.6 is the Red on Black ware of likely Cypriot origin discussed in the text); Principal components analysis of the KH3 group illustrating (c) the distribution of KH3A and KH3B groups (KH3B.1−3B.7) and the apparent compositional homogeneity of KH3A; and (d) following removal of KH3B groups, the decomposition of KH3A into distinct compositional and typological groups (KH3A.1−3A.5+) shown here linked to a typical ware for each (not to scale); (e) Principal components analysis of the Hodos et al. (2005) NAA dataset. Note the close structural similarity with that of the current study (a, above); (f) cluster analysis (Ward's Method) of the Hodos et al. (2005) NAA dataset showing both the original sample numbers and their reorganized compositional groups discussed in the text as Hodos 1−4, and summarized in Table 5.

Table 3
The Kinet NAA dataset organized into four principal compositional groups and their major subsets giving group identification, number of samples in each group, average value and % coefficient of variation (CV)

ppm	KH1.1 (n = 44)		KH1.2 (n = 12)		KH1.3 (n = 30)		KH2.1 (n = 57)		KH2.2 (n = 45)	
	Avg.	CV	Avg.	CV	Avg.	CV	Avg.	CV	Avg.	CV
As	14.14	32.99	9.42	53.86	9.10	40.33	7.23	21.72	8.24	22.48
Ba	169.57	38.41	132.83	45.57	229.37	31.26	319.12	16.27	269.13	22.39
Ca%	4.95	37.27	8.62	47.42	9.74	25.52	10.14	13.93	10.93	14.08
Ce	32.68	22.00	20.42	41.00	29.63	22.95	41.84	7.90	33.54	9.71
Co	95.22	18.75	84.63	23.42	51.62	21.00	32.53	7.40	29.54	9.10
Cr	1580.64	32.82	3512.50	73.72	1742.70	112.55	398.49	27.72	406.11	48.58
Cs	2.12	36.61	1.63	35.80	2.72	40.28	3.99	18.73	3.16	22.42
Eu	0.65	25.07	0.48	39.26	0.73	18.40	1.01	12.55	0.86	14.60
Fe%	5.67	14.88	5.96	16.11	5.10	13.54	4.99	8.66	4.89	11.09
Hf	2.29	27.05	1.40	39.48	2.09	23.57	2.93	12.94	2.55	14.69
K%	1.04	47.12	0.51	92.45	1.35	24.72	1.60	35.39	1.64	34.44
La	16.73	21.07	10.84	33.60	15.73	23.45	21.77	7.36	17.68	7.56
Lu	0.18	29.46	0.16	32.52	0.22	25.04	0.29	7.97	0.27	11.61
Na%	0.33	34.73	0.32	42.22	0.55	42.11	0.79	19.67	0.91	14.70
Nd	15.27	21.80	11.58	20.97	16.03	16.01	20.18	13.42	17.46	14.68
Rb	36.73	27.51	22.58	45.29	40.30	21.18	62.33	14.75	52.30	16.49
Sb	3.21	37.05	1.18	63.39	1.04	45.70	0.91	15.26	0.81	13.06
Sc	12.40	16.20	14.33	15.04	16.74	25.65	19.08	9.13	19.86	15.43
Sm	2.93	20.51	2.05	36.00	3.01	20.19	4.11	7.01	3.51	6.84
Ta	0.63	66.39	0.31	127.84	0.73	50.59	0.87	56.06	0.63	85.26
Tb	0.25	128.62	0.13	198.00	0.19	158.41	0.57	71.01	0.33	120.19
Th	4.35	23.46	2.83	39.68	4.12	22.56	6.31	9.00	4.88	9.00
U	1.72	27.57	0.71	67.96	1.10	118.27	1.21	51.60	1.44	56.22
Yb	1.25	22.38	1.03	31.79	1.53	20.07	2.06	7.66	1.96	8.81
Zn	74.70	24.48	90.08	38.60	97.23	28.91	99.51	16.02	96.85	14.29

	KH2.3 (n = 2)		KH2.6 (n = 4)		KH3A (n = 39)		KH3B (n = 53)		KH4 (n = 4)	
	Avg.	CV	Avg.	CV	Avg.	CV	Avg.	CV	Avg.	CV
As	12.00	0.00	10.00	17.32	15.46	49.94	10.23	45.21	3.00	27.22
Ba	330.00	8.57	119.67	14.96	447.95	36.95	434.53	20.11	90.00	124.06
Ca%	16.00	8.84	8.63	13.82	5.11	46.53	6.66	31.92	3.38	8.85
Ce	32.50	2.18	22.67	9.18	72.13	19.40	79.43	15.70	20.75	18.19
Co	22.50	9.43	26.67	4.33	33.29	20.52	19.59	22.60	43.25	3.47
Cr	262.50	23.97	182.33	6.86	432.67	58.12	130.39	39.13	246.00	33.37
Cs	4.00	31.82	2.37	6.45	11.06	79.69	10.34	38.76	−	−
Eu	0.84	0.85	0.66	18.17	1.33	15.72	1.30	14.04	0.75	28.51
Fe%	3.23	10.51	5.43	2.38	5.67	11.84	4.59	11.47	7.60	9.71
Hf	2.00	7.07	1.70	15.56	4.52	23.55	4.79	22.95	1.33	67.89
K%	2.30	12.30	1.37	18.41	2.58	31.38	2.88	31.15	0.28	200.00
La	18.10	7.81	12.60	6.92	36.49	17.53	40.98	14.87	9.83	17.97
Lu	0.20	14.14	0.24	4.75	0.41	14.47	0.39	11.62	0.27	17.89
Na%	0.64	17.68	1.45	2.62	0.69	36.18	0.57	32.78	1.03	40.83
Nd	19.00	0.00	13.67	11.18	28.95	16.45	32.58	13.93	20.25	21.10
Rb	54.50	16.87	39.00	11.18	122.18	24.64	138.09	19.29	20.50	75.20
Sb	1.20	47.14	0.90	0.00	1.75	49.34	1.40	28.91	−	−
Sc	11.35	6.85	26.47	4.00	20.87	13.37	16.67	13.97	41.10	2.31
Sm	3.03	1.64	2.75	3.78	6.36	15.13	6.60	13.97	2.47	15.13
Ta	0.70	20.20	−	−	1.39	50.33	1.57	36.45	0.38	200.00
Tb	0.50	0.00	0.33	173.00	0.80	51.50	0.85	49.95	0.23	200.00
Th	5.75	6.15	2.77	4.17	11.42	22.35	14.79	23.48	2.43	20.03
U	1.25	16.97	1.50	46.67	1.75	56.16	3.09	35.10	−	−
Yb	1.50	0.00	1.87	3.09	2.89	15.02	2.82	13.89	1.93	16.08
Zn	69.50	11.19	130.00	7.69	121.31	15.87	109.74	12.46	66.25	11.12

include Red Lustrous Wheel made (KH3A.4 and 4+) and "Orientalizing" wares (KH3A.5 and 5+). The dominance of two groups (KH3A.1 and KH3B.4) in the KH3 sample suggests the relative importance of two major production centers within this general class of Kinet imports.

The fourth group (KH4) represents a typologically well known LBA type of handmade Cypriot white slipped ware ("milk bowls") (Fig. 4d 1−4). The typological and compositional homogeneity of KH4 (highest relative scandium concentrations of the sample with generally lower
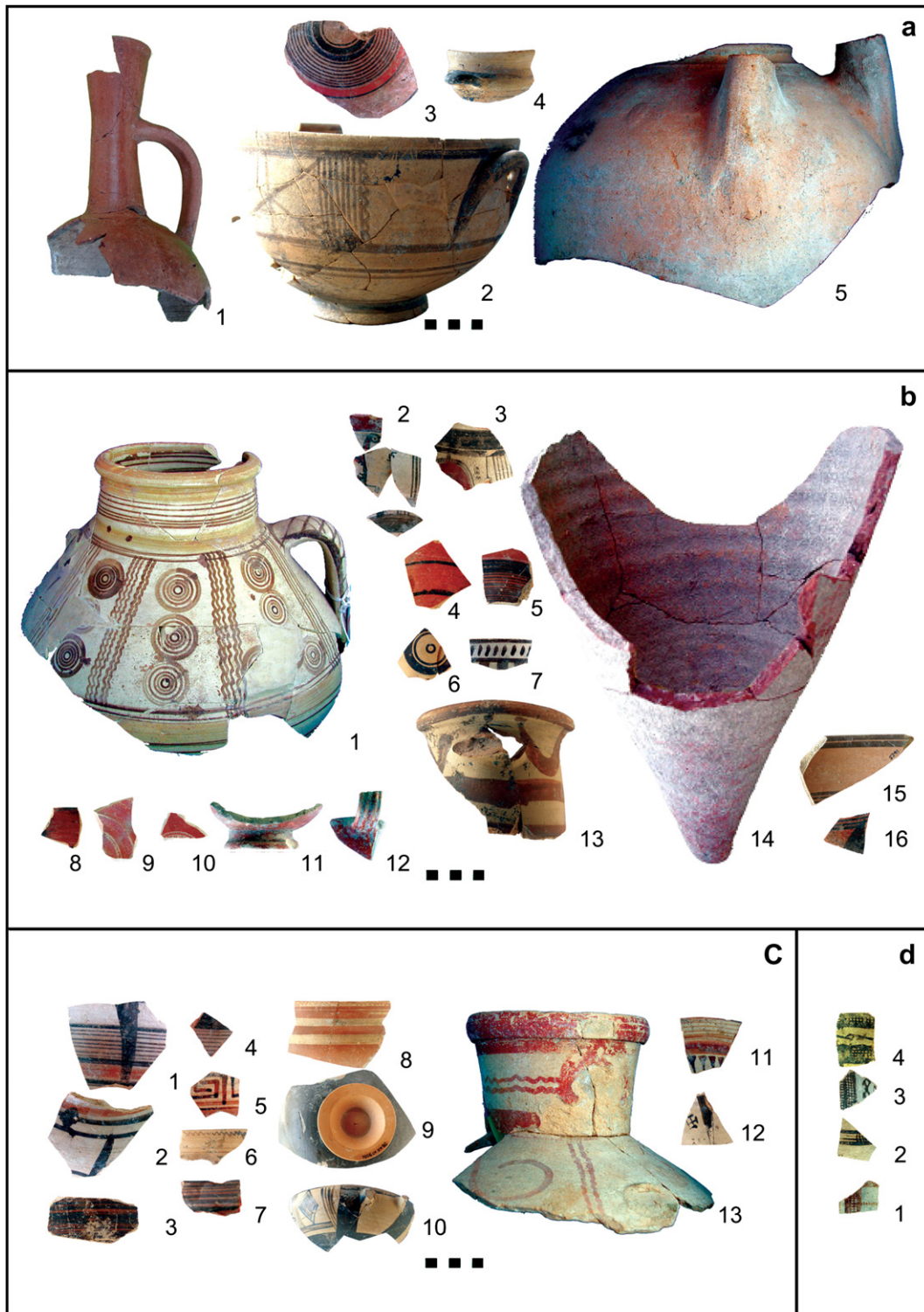
Fig. 4. Kinet types. Examples of the typological range of each major compositional group (a = KH1 subsets; b = KH2 and subsets; c = KH3 and major non-core subsets; d = KH4 Cypriot LBA white slipped "milk bowls"). Note aia prefix refers to the Anatolian Iron Age catalogue number. KH1.1: a1 (aia 788), a2 (aia 758), a3 (aia 1653); KH1.3: a4 (aia 1702), a5 (aia 803); KH2.1: b1 (aia 801), b4 (aia 1600), b5 (aia 1549), b6(aia 1595), b8 (aia 1601), b9 (aia 779), b10 (aia 777), b 11 (aia 774), b 12 (aia 773), b 14 (aia 771); KH2.2: b2 (aia 760); b3 (aia 1652), b13 (aia 1684); KH2.5: b7 (aia 764); KH2.6: (Cypriot (Troodos?)) Black on Red ware) b15 (aia 1625), b16 (aia 1664); KH3B.1: c1 (aia 794), c2 (aia 799), c3 (aia 1679), c4 (aia 798), c7 (aia 1555); KH3B.101: c5 (aia 1700); KH3B.2: c10 (aia 1694); KH3B.4: c6 (aia 1677), c8 (aia 1676), c9 (aia 1678); KH3B.6: c11 (aia 1701), c12 (aia 1704), c13 (aia 806); KH4 (Cypriot white slip "milk bowls"): d1 (aia 1718), d2 (aia 1719), d3 (aia 1720), d4 (aia 1721).

Table 4
Non-core subsets of KH 3B giving group identification, number of samples in each group, average value and % coefficient of variation (CV)

ppm	KH3B.1 ($n = 4$)		KH3B.1i ($n = 5$)		KH3B.1ii ($n = 2$)		KH3B.1iii ($n = 3$)		KH3B.2 ($n = 4$)		KH3B.3 ($n = 3$)	
	Avg.	CV	Avg.	CV	Avg.	CV	Avg.	CV	Avg.	CV	Avg.	CV
As	13.75	9.15	16.20	42.63	9.50	7.44	9.00	0.00	7.00	30.86	6.00	0.00
Ba	317.50	17.70	360.00	14.83	280.00	5.05	503.33	25.24	647.50	20.19	366.67	11.02
Ca%	4.90	15.72	7.50	41.88	6.15	10.35	3.97	73.60	4.90	27.53	10.23	31.46
Ce	66.25	7.83	55.40	5.50	56.50	1.25	95.33	15.36	80.00	3.39	63.67	9.47
Co	29.50	5.87	37.48	28.74	28.50	2.48	19.33	2.99	26.25	10.02	32.67	14.14
Cr	896.25	43.58	452.80	19.94	733.50	4.53	134.20	25.88	175.50	6.81	271.67	25.95
Cs	4.78	2.01	10.06	55.02	4.90	0.00	15.17	56.37	10.95	32.17	8.67	20.94
Eu	1.35	7.41	1.05	14.63	1.15	6.15	1.63	9.35	1.40	5.83	1.27	12.06
Fe%	5.05	4.78	5.09	8.75	5.01	2.26	5.23	12.33	5.64	4.58	5.59	9.61
Hf	4.25	11.28	3.82	12.47	3.75	1.89	5.80	12.07	4.55	19.70	3.03	1.90
K%	2.05	11.61	2.46	40.30	3.35	10.55	2.77	51.92	3.28	25.23	2.63	19.11
La	34.75	5.62	27.74	8.58	29.65	2.15	49.27	10.39	40.15	0.52	33.70	6.43
Lu	0.39	2.96	0.32	5.61	0.37	1.94	0.46	8.70	0.43	4.77	0.37	1.57
Na%	0.68	4.21	0.56	39.36	0.79	6.31	0.57	8.88	0.93	31.32	0.62	46.28
Nd	28.00	13.98	24.40	16.55	28.00	0.00	39.00	6.78	31.75	9.05	29.67	1.95
Rb	90.75	6.63	94.80	17.26	91.50	6.96	150.00	6.67	155.00	11.17	143.33	4.03
Sb	1.05	16.50	1.14	38.03	1.05	6.73	1.33	31.22	1.60	51.03	0.67	8.66
Sc	18.23	3.94	18.60	9.49	18.45	1.92	19.37	5.94	21.55	4.26	21.67	6.15
Sm	6.40	3.46	5.09	7.32	5.37	0.92	7.80	14.68	6.69	3.47	5.68	6.61
Ta	1.23	38.51	1.18	21.10	1.20	11.79	1.63	43.00	1.73	18.56	1.03	89.92
Tb	0.85	28.01	0.86	13.26	0.90	15.71	1.00	0.00	0.63	115.65	0.63	89.78
Th	8.98	5.26	8.26	5.59	8.70	0.00	16.33	3.53	14.75	11.58	11.00	9.09
U	0.85	73.97	3.78	88.33	1.55	4.56	3.07	21.22	2.25	71.34	0.83	173.21
Yb	2.85	7.30	2.32	8.29	2.30	0.00	3.17	9.12	2.88	3.33	2.53	4.56
Zn	105.50	18.98	117.60	11.68	110.00	0.00	104.00	9.99	135.00	12.83	130.00	7.69

	KH3B.4 ($n = 15$)		KH3B.5 ($n = 2$)		KH3B.5i ($n = 2$)		KH3B.6 ($n = 6$)		KH3B.7 ($n = 2$)	
	Avg.	CV	Avg.	CV	Avg.	CV	Avg.	CV	Avg.	CV
As	22.27	25.54	10.00	42.43	14.50	92.66	13.50	29.91	21.00	20.20
Ba	480.67	20.30	220.00	6.43	415.00	8.52	528.33	10.80	575.00	82.39
Ca%	5.59	30.31	0.60	0.00	4.35	102.41	4.62	25.61	1.55	41.06
Ce	73.40	8.30	90.00	25.14	68.00	16.64	95.67	9.10	112.50	8.17
Co	34.33	14.80	32.50	15.23	37.50	1.89	19.67	8.90	33.50	10.55
Cr	349.40	27.30	286.00	11.37	481.00	29.40	161.50	8.51	132.50	0.53
Cs	17.21	66.77	3.60	43.21	12.30	54.04	11.07	12.61	10.20	11.09
Eu	1.37	9.45	1.40	10.10	1.15	6.15	1.40	9.04	1.90	14.89
Fe%	6.10	7.16	6.93	10.93	5.85	13.30	4.27	4.38	5.66	22.49
Hf	4.71	12.98	6.90	24.60	4.60	3.07	5.18	9.08	6.05	36.23
K%	2.83	27.61	1.55	22.81	2.15	9.87	3.17	32.37	2.40	23.57
La	38.35	8.02	41.60	8.16	30.65	5.31	48.92	8.00	58.40	13.32
Lu	0.43	8.33	0.55	6.49	0.40	0.00	0.47	10.58	0.45	3.14
Na%	0.62	29.53	0.73	46.49	0.65	15.23	0.97	11.23	0.38	47.14
Nd	28.27	11.54	37.50	1.89	29.00	14.63	34.33	18.02	36.50	9.69
Rb	147.33	13.44	72.50	22.43	115.00	6.15	180.00	11.11	135.00	5.24
Sb	2.56	11.98	0.90	15.71	1.15	6.15	1.42	8.25	3.05	44.05
Sc	22.71	6.27	26.15	2.97	22.45	3.46	13.25	4.74	18.35	15.80
Sm	6.56	6.83	7.40	5.64	5.84	0.97	8.19	9.66	8.96	3.31
Ta	1.47	31.10	3.35	27.44	1.40	60.61	2.13	28.07	1.60	26.52
Tb	0.77	64.59	0.80	0.00	0.51	138.62	1.38	8.45	1.15	18.45
Th	13.90	19.04	8.40	15.15	9.50	7.44	22.42	7.58	16.50	12.86
U	2.19	43.47	1.15	6.15	1.75	12.12	3.80	13.11	2.55	41.59
Yb	3.11	8.20	3.80	7.44	2.80	0.00	3.62	11.12	3.40	8.32
Zn	126.67	10.19	115.00	6.15	155.00	22.81	92.50	15.72	135.00	15.71

concentrations of trace elements and rare earths) best match NAA results for LBA white slipped ceramics and geological sediments from the southern region of the Troodos massif that dominates the central western region of Cyprus (Gomez et al., 2002).

6. Chronology

The relationship between geochemical groups and cultural time at the site can be summarized by plotting the frequency of the main KH groups for each phase (Figs. 5 and 6). For the

Table 5
Core subsets of KH 3A giving group identification, number of samples in each group, average value and % coefficient of variation (CV)

ppm	KH3A.1 ($n = 16$)		KH3A.2 ($n = 8$)		KH3A.3 ($n = 4$)		KH3A.4 ($n = 2$)	
	Avg.	CV	Avg.	CV	Avg.	CV	Avg.	CV
As	7.56	19.29	9.13	36.79	9.50	13.59	7.50	9.43
Ba	418.13	13.28	442.50	15.88	355.00	13.11	330.00	8.57
Ca%	6.48	13.83	7.24	22.38	9.48	13.28	6.00	4.71
Ce	77.25	2.93	71.75	3.05	66.75	7.38	76.00	5.58
Co	18.63	8.05	17.25	5.14	14.25	3.51	24.50	14.43
Cr	101.07	4.80	96.96	12.30	84.05	4.99	124.50	3.98
Cs	9.00	5.05	8.16	6.83	6.38	4.51	9.10	3.11
Eu	1.28	8.17	1.21	12.29	1.01	6.94	1.25	5.66
Fe%	4.65	2.98	4.37	2.07	3.83	2.61	5.35	0.66
Hf	4.49	5.45	4.16	6.66	3.95	13.15	4.35	8.13
K%	3.30	21.74	3.06	16.83	2.10	10.29	2.30	18.45
La	40.01	2.52	37.55	2.45	33.48	4.64	39.05	1.27
Lu	0.40	3.46	0.36	5.75	0.34	9.90	0.36	17.93
Na%	0.56	10.67	0.57	8.52	0.51	10.72	0.20	0.00
Nd	34.25	10.42	29.00	7.60	29.00	5.63	30.00	4.71
Rb	144.38	6.18	131.25	6.36	107.50	8.91	140.00	10.10
Sb	1.67	7.16	1.54	7.73	1.45	11.95	1.10	0.00
Sc	16.75	2.45	16.05	8.84	13.68	3.89	18.70	3.03
Sm	6.53	1.86	6.13	3.04	5.61	4.99	6.44	2.97
Ta	1.46	22.98	1.56	27.57	1.18	24.44	1.15	43.04
Tb	0.94	20.82	0.85	45.78	0.53	67.21	0.75	9.43
Th	13.75	4.20	12.75	3.63	11.00	7.42	14.00	0.00
U	3.02	17.03	2.53	14.63	2.78	13.60	2.60	5.44
Yb	2.71	5.53	2.54	4.68	2.40	6.80	2.80	5.05
Zn	113.06	8.52	107.63	11.79	110.50	11.95	92.50	5.35

ppm	KH3A.4+ ($n = 2$)		KH3A.5 ($n = 5$)		KH3A.5+ ($n = 2$)	
	Avg.	CV	Avg.	CV	Avg.	CV
As	7.00	20.20	17.80	17.50	9.00	31.43
Ba	460.00	6.15	506.00	14.56	525.00	9.43
Ca%	5.70	9.92	7.62	5.20	7.00	4.04
Ce	91.00	3.11	77.80	3.68	75.00	5.66
Co	19.50	3.63	20.40	4.38	20.50	3.45
Cr	130.50	1.63	148.60	3.35	148.00	5.73
Cs	7.10	3.98	16.20	6.76	16.00	0.00
Eu	1.45	14.63	1.30	9.42	1.35	5.24
Fe%	4.68	1.06	4.18	3.35	4.79	7.97
Hf	5.05	4.20	5.66	5.39	5.10	5.55
K%	3.45	10.25	2.14	34.43	2.75	2.57
La	47.15	0.15	39.42	1.37	39.50	3.58
Lu	0.38	3.72	0.39	5.53	0.41	12.22
Na%	0.41	1.75	0.55	1.98	0.56	1.27
Nd	34.00	8.32	30.40	4.99	35.00	4.04
Rb	130.00	0.00	114.00	4.80	135.00	5.24
Sb	0.75	9.43	0.92	9.09	0.90	0.00
Sc	16.05	2.20	16.58	3.06	18.50	3.82
Sm	7.46	2.09	6.09	1.34	5.90	1.44
Ta	1.55	41.06	1.46	30.09	1.16	140.20
Tb	1.25	16.97	0.40	138.07	0.01	141.42
Th	14.00	0.00	14.20	3.15	16.50	4.29
U	2.70	26.19	2.54	26.93	3.30	4.29
Yb	2.95	2.40	2.86	3.99	2.65	2.67
Zn	115.00	6.15	112.00	7.47	105.00	6.73

LBA and EIA phases (local) KH1 classes dominate, with KH2 and KH3 (imported) classes forming a small but constant component of these phases. The beginning of the MIA is marked by both a large increase in the total number of samples and a dramatic shift in the relative proportion of classes. More than 35% of all KH2 wares occur in this phase, and around 30% of all KH1 wares. The proportion of KH3 remains relatively small at around 10% of the total KH3 sample. These relative proportions are maintained in the next MIA phases though total numbers decrease. By the LIA phases, the situation is completely reversed with the overwhelming bulk of the sample now KH3 wares. By the Hellenistic phase, with
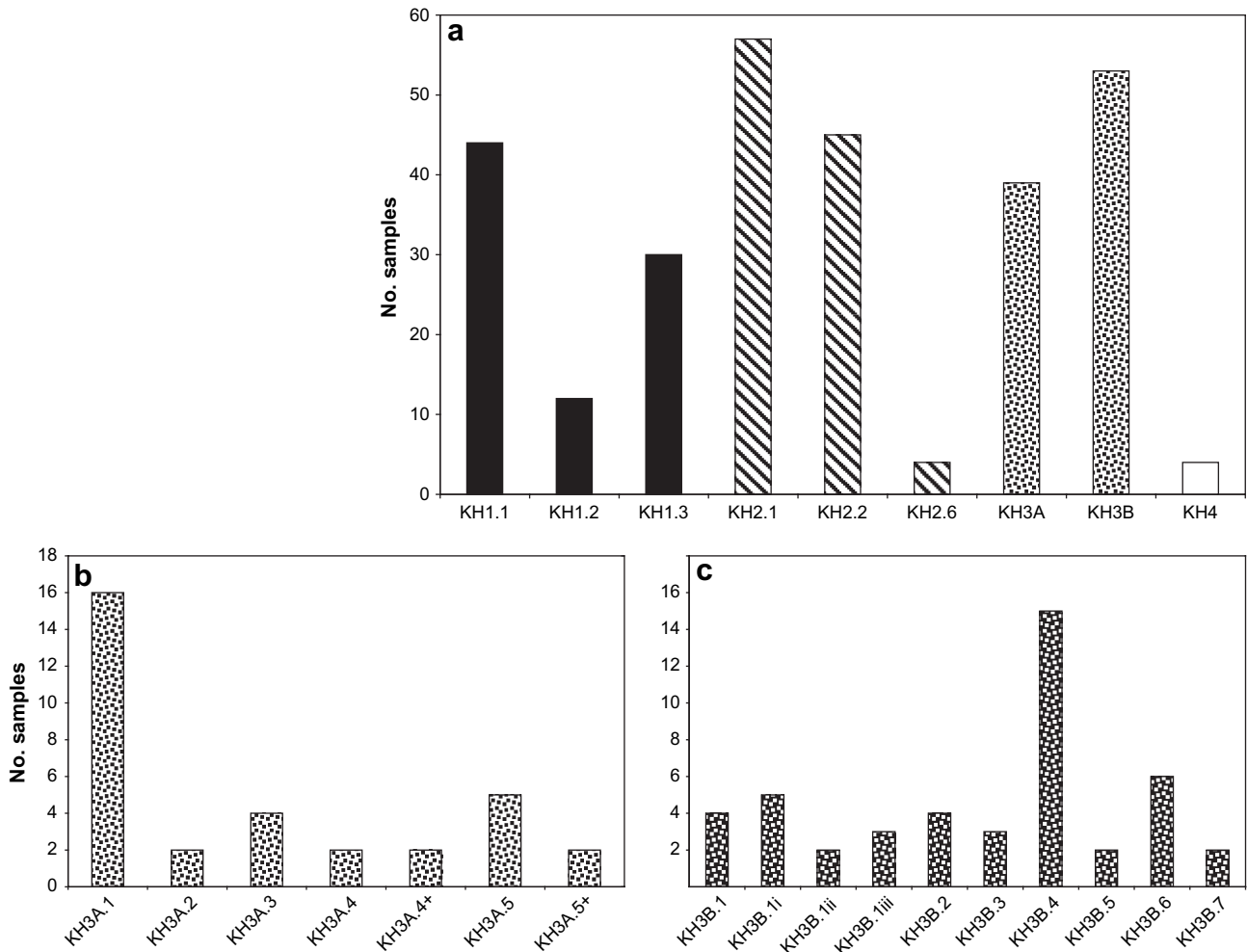
Fig. 5. Frequency histogram for the main compositional groups of the study (a) showing overall even representation of the main KH groups. In contrast, frequency plots for the groups identified within KH3A (b) and 3B (c) show two dominant groups (KH3A.1 and KH3B.4), that infer the importance of two distinct production centers within the KH3 class of imports.

a greatly diminished total sample, the assemblage is again dominated by KH2 imports (Eastern Sigillata A types: Fig. 4b 8–12).

A more detailed examination of frequency distributions for each KH class and its subsets reveals further complexities in these patterns. While the KH1 group's fabrics have little to differentiate them, the frequency plot shows that KH1.2 is only present in the LBA and EIA phases lending some weight to the role of potter choice in differentiating this group (Fig. 7a). Given the shift away from Hittite production techniques at the end of the LBA, this may provide an independent measure of local changes in technological style.

For the KH2 subsets, the largest total quantities and greatest diversity of classes occur in the MIA phases (Fig. 7b). Exceptions are the restricted range of KH2.3 (LBA II-early MIA) and KH2.6 (early MIA) suggesting that the KH2 subsets also reflect significant temporal differences. KH2.1 and 2.2 wares also continue (albeit at low levels) across almost all other phases of the site.

For the KH3 core subsets (KH3A.1–5+), a different chronological pattern is evident (Fig. 7c). The majority occur in

Late Iron Age phases but KH3A.4 (red lustrous wheel made ware) is restricted to LBA II phases, and KH3A.4+ (a red lustrous (?)variant) is restricted to terminal EIA phases. Of the LIA classes, one (KH3A.3) is present from as early as the late MIA. The frequency distributions for the non-core KH3 classes (KH3B.1–3B.7) are based on very small group memberships, however, there does seem to be a chronological distribution for some classes: KH3B.1 first appears in the EIA, reaches a peak in the MIA and dwindles in the LIA (Fig. 7d). Another class (KH3B.6), represented in the LIA, reaches its peak in the Hellenistic phases; while a third class (KH3B.2) extends from the early MIA to the Hellenistic. The sources of exotic wares changed dramatically over time, with each phase having a unique pattern of exchange relationships. The LIA (phase 7) has the greatest density of these exchange relationships as seen by the diversity present in the KH3A groups.

7. Comparison with previous NAA work at Kinet

Definition of the local, regional and long-distance compositional groups present in a broad cross-section of the Kinet
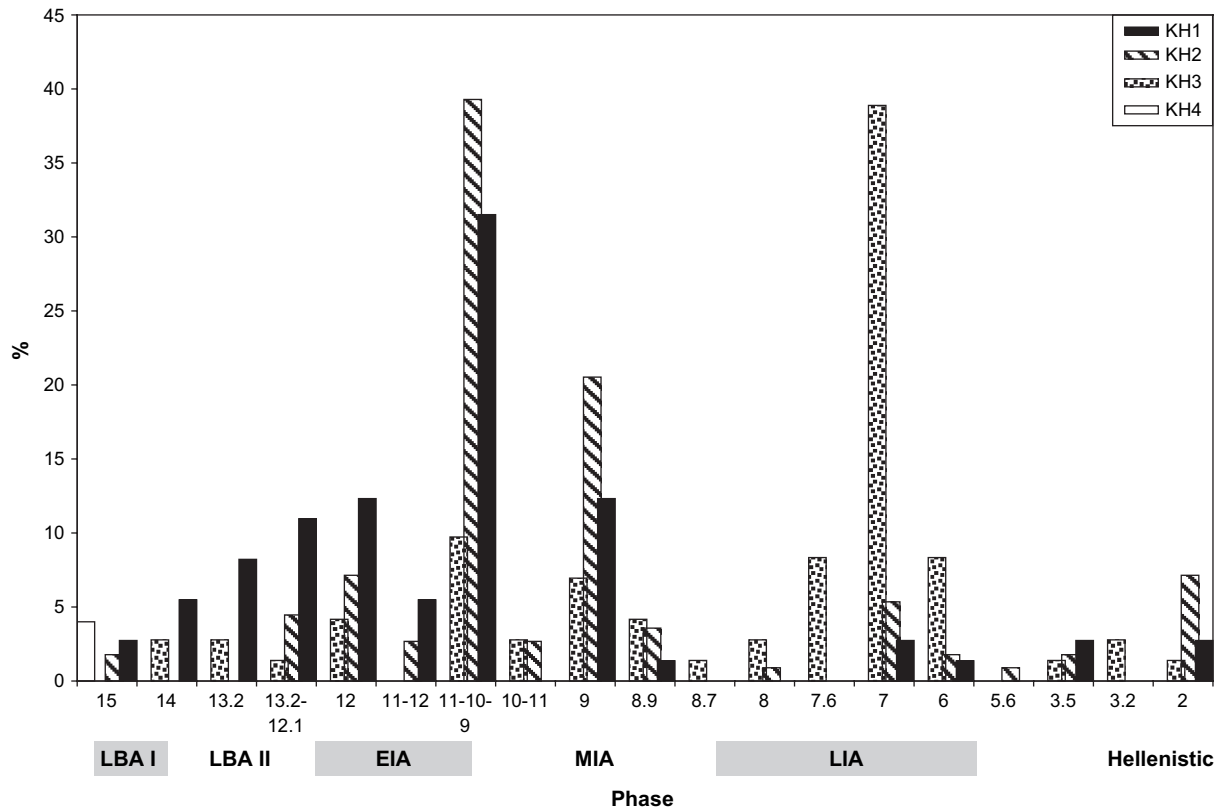
Fig. 6. Frequency histogram of distribution of main compositional groups organized by chronological phases (each group summed to 100%).

ceramic corpus provides an excellent opportunity to contextualize previous, more narrowly focused NAA studies at this site. For Kinet, two studies have been conducted to distinguish local from imported ceramics. One analyzed painted wares of the 8th and 7th centuries B.C. as part of an investigation on the effects of occupation by Neo-Assyrians on local ceramic production (Hodos et al., 2005). The other focused on glazed ceramics of the 13th century A.D. to determine the range of medieval trade wares in maritime circulation (Blackman and Redford, 2005).

Both studies used NAA of ceramic samples in conjunction with typological, contextual and (for the Hodos et al. study) petrographic data to distinguish local from imported wares. For the Hodos et al. study, a full NAA dataset was available for reanalysis (Table 6), while for the Blackman and Redford study only summary results were available (Table 7). Both NAA datasets varied in the elements that were reported and that could be compared with the present study.

In the Hodos et al. (2005) study, several elemental groups were identified from a sample population of thirty-nine. The study included wasters associated with two kilns from contexts that bracketed their period of interest. The kiln wasters formed part of a group that was chromium rich with an abundance of a mineral (serpentinite) typical of the adjacent ophiolitic coastal range. This group was considered local to the site while the majority of the remaining sample, though broadly similar, was designated as "regional." A small number of typologically linked samples (black on red banded bowl fragments) with a distinct igneous fabric were suggested to be of possible Cypriot origin.

The larger Blackman and Redford study of one hundred seventy-nine samples distinguished five compositional groups. Like the Hodos et al. study, they identified a chromium-rich group that included kiln waste from Kinet (no actual kiln structures were identified in the medieval levels). This group (B&R 4), considered consistent with ophiolitic compositions of the hinterland geology, could not be differentiated from analysis of production debris from a contemporary site 20 km distant (location unspecified). A second group (B&R 2) that included kiln wasters from Port St Simeon (al-Mina), was assigned an origin at that site. Two further groups, (results only published for one (B&R 3)), were assigned to undefined locations on the "Cilician coast" based on general elemental similarities to the regional signature for Kinet. A final group (B&R 1) was assigned an Aegean or Cypriot origin.

A few caveats need to be made in undertaking comparison between NAA datasets from different facilities. First, there is usually a close correlation between number of elements and number of elemental groups that can be resolved (Grave et al., 2005). In datasets where number and selection of elements vary it is necessary to reduce all datasets to a smaller pool of common elements, a situation likely to involve some loss of group resolution. Second, the application of correction factors based on comparison of experimental results for standard reference materials has been suggested as a necessary step for robust cross-facility comparisons (Hein et actual., 2002). In practice, insensitivity to minor differences in sample preparation, broad adoption of similar counting procedures, and the use of high dimensional, multivariate analysis has been
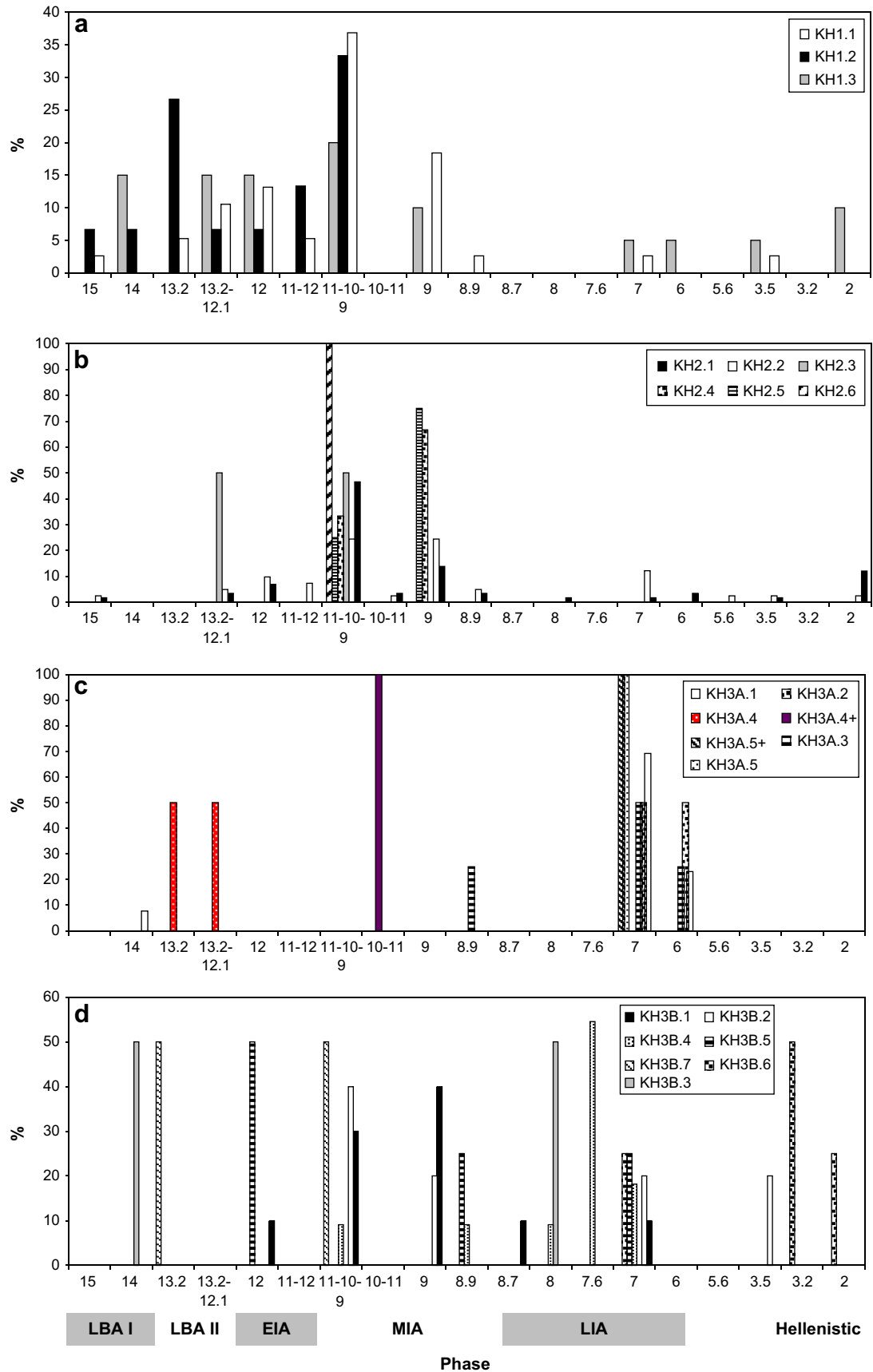
Fig. 7. Frequency histograms of compositional subsets for KH1 (a), KH2 (b), KH3A core (d) and KH3B (e) organized by chronological phases.

Table 6
Summary of the Hodos et al. (2005) NAA dataset organized by four principal compositional groups and their subsets giving group identification, number of samples in each group, average value and % coefficient of variation (CV)

ppm	Hodos 1 (n = 8)		Hodos 1.1 (n = 2)		Hodos 2 (n = 7)		Hodos 2.1 (n = 3)	
	Avg.	CV	Avg.	CV	Avg.	CV	Avg.	CV
Ca%	10.19	25.40	3.18	18.68	11.15	14.19	15.10	14.34
Ce	56.98	7.70	80.55	1.32	52.31	8.61	42.37	9.45
Co	30.94	10.43	28.25	4.76	27.83	10.40	24.97	11.33
Cr	286.13	16.17	152.50	5.10	274.57	20.31	264.67	6.14
Cs	4.66	7.66	4.28	12.07	3.88	11.58	3.10	13.05
Eu	1.13	9.38	1.54	4.15	0.99	4.34	0.76	2.75
Fe%	5.04	12.28	5.25	0.27	4.39	8.32	3.31	2.18
Hf	3.78	9.77	5.09	6.54	3.25	8.33	2.66	7.55
K%	1.98	21.97	1.59	4.02	1.93	25.19	1.66	20.63
La	25.53	7.34	35.00	0.40	21.87	8.34	17.57	6.24
Lu	0.32	7.09	0.39	10.88	0.27	5.51	0.22	6.84
Na%	0.80	16.96	0.43	1.66	0.70	22.52	0.60	3.83
Rb	78.05	6.52	73.35	15.71	67.34	13.79	51.70	7.71
Sc	18.14	12.88	17.85	1.19	16.13	8.71	11.80	3.06
Sm	4.84	7.60	6.95	1.83	4.14	5.79	3.24	3.12
Ta	0.90	10.63	1.39	6.10	0.76	9.88	0.56	12.50
Tb	0.90	30.48	1.09	28.54	0.59	10.89	0.49	15.41
Th	8.19	5.83	10.85	0.65	7.04	8.59	5.86	2.81
U	2.29	7.47	2.03	1.75	2.02	3.07	1.94	8.79
V_2O	4.89	11.20	5.21	2.17	4.33	7.85	3.27	1.33
Yb	2.42	5.68	3.11	6.37	2.16	2.70	1.72	2.35
Zn	99.68	17.52	106.40	52.63	86.64	16.25	73.90	8.48

	Hodos 3 (n = 6)		Hodos 3.1 (n = 4)		Hodos 4 (n = 7)	
	Avg.	CV	Avg.	CV	Avg.	CV
Ca%	11.95	8.96	8.03	15.51	6.50	26.62
Ce	40.90	10.08	39.18	18.50	47.38	15.46
Co	28.78	14.92	28.33	7.02	87.20	19.17
Cr	311.83	43.75	179.25	22.58	1168.80	12.12
Cs	3.12	17.07	2.19	14.80	2.23	24.95
Eu	0.95	5.59	0.77	3.74	0.72	4.21
Fe%	4.94	6.21	5.51	7.90	5.91	9.48
Hf	2.75	7.91	2.24	4.30	2.53	3.37
K%	1.66	24.35	1.45	10.95	1.38	23.55
La	17.08	7.11	13.58	6.38	17.68	7.50
Lu	0.29	5.77	0.27	6.76	0.20	8.90
Na%	0.99	16.46	1.46	13.40	0.42	19.13
Rb	59.83	20.36	45.90	14.83	42.08	23.23
Sc	19.90	6.30	25.95	8.02	13.20	7.85
Sm	3.63	6.68	3.02	3.53	3.35	5.39
Ta	0.54	12.29	0.44	8.30	0.69	8.60
Tb	0.63	10.26	0.61	6.77	0.69	21.91
Th	5.45	14.49	3.46	6.66	6.60	7.62
U	2.60	14.32	1.95	11.38	2.42	12.53
V_2O	4.87	6.01	5.48	6.95	5.73	9.55
Yb	2.15	5.10	2.02	5.59	1.49	7.10
Zn	98.18	10.31	125.75	12.36	76.50	13.29

argued to mitigate the importance of measurement differences between NAA laboratories (Glascock and Neff, 2003). Even where a direct numerical comparison may be suspect, PCA of two different datasets for the same assemblage can be sufficiently similar to allow comparison of structural features and element/sample relationships (Grave et al., 1996). For the present study a measure of cross facility variation was not possible because standards data were either omitted (Hodos et al., 2005) or were obsolete (the Blackman and Redford, 2005 study published results for a standard (SRM1633a) that has

been unavailable for several years). Notwithstanding the potential offsets involved in comparing these three datasets we note that as all three are based at the same site we could expect a higher degree of confidence in cross-dataset correlations than might otherwise be the case.

To facilitate comparison with the present study the Hodos et al. (2005) dataset was reanalyzed using a combination of hierarchical clustering (Ward's Method) and validation by PCA/CVA to identify four major groups and three subsets (Fig. 3f). Comparison of the PCA projection for the Hodos

Table 7
Blackman and Redford (2005) NAA data table p. 186 table 3, giving group identification, number of samples in each group, average value and % coefficient of variation (CV)

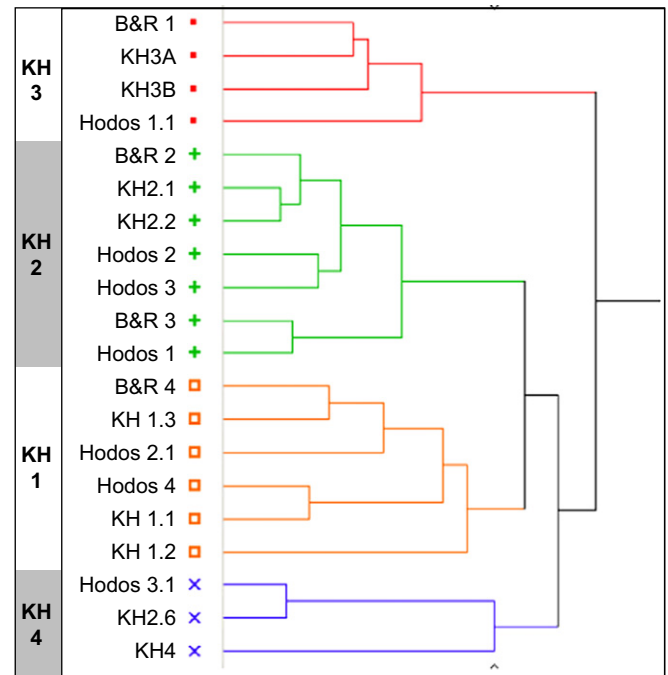| ppm	B&R 1 (n = 30)		B&R 2 (n = 47)		B&R 3 (n = 10)		B&R 4 (n = 57)	
	Avg.	CV	Avg.	CV	Avg.	CV	Avg.	CV
Ba	575	17.4	315	25.2	299	32.7	308	29.5
Ca%	3.43	23.3	13.3	15.3	11.3	20	11.2	14.8
Ce	77.1	2.8	38.4	7.9	56.4	4.6	32	9.3
Cr	165	6	406	13	486	16.9	779	16.7
Cs	8.42	6.9	3.09	13.1	3.63	8.7	2.5	15.5
Eu	1.34	2	0.943	6	1.09	5.8	0.75	9.8
Fe%	4.99	4.6	4.4	10.4	4.74	5.4	4.77	5.8
Hf	5.1	9	3.32	10.4	3.67	6.7	2.62	12.2
K%	2.77	6.3	1.29	14.3	1.51	9.5	0.852	16.5
La	41.8	2.5	21.6	9.1	30.4	5.9	17.9	8.6
Lu	0.411	10.3	0.305	13.7	0.343	15.2	0.249	15.3
Na%	1.11	6.6	0.988	15.3	0.714	12.7	0.596	32.6
Nd	32.7	10.8	16.1	25.7	22.8	15.3	13	16.8
Rb	163	6	59.9	15.8	68.6	8.4	42.7	17.4
Sc	19.6	4.6	17	9.8	17.3	5.7	15.1	8.8
Sm	6.38	5.4	3.83	8	4.89	8.5	3.01	8.2
Sr	–	–	468	20.2	401	17.4	381	17.2
Ta	1.81	45.3	0.698	18.4	1.06	12.8	0.631	20.3
Tb	1.02	12	0.599	15.9	0.766	19.2	0.473	18.9
Th	13.5	2.9	5.67	11.2	7.63	4.9	4.63	10.4
U	1.43	33.1	0.94	36.3	1.26	27.5	0.77	36.7
Yb	3.08	7.8	2.16	9.6	2.35	4.8	1.68	11.6
Zn	110	10.2	89.2	17.5	102	11	74.6	17.4

Fig. 8. Cluster analysis (Ward's Method) of group means and common elements for the Hodos et al. (2005) NAA dataset, the Blackman and Redford (2005) NAA dataset and for the major groups and subsets of the present study. The result of this analysis indicates good overall agreement between the three studies on membership of each of the three major KH groups, in addition to a good fit between subsets of Black on Red ware in the Hodos et al. (2005) dataset (Hodos 3.1) and the present study (KH2.6).

et al., dataset with that of the present study shows that Hodos group 4 is structurally and compositionally directly comparable to the local KH1.1 group (Fig. 3a,e). The remaining Hodos groups lie along the non-local KH4−KH2−KH3 plane.

Incorporation of the Blackman and Redford summary dataset for comparison required reduction of both the Hodos et al. and KH datasets to group means and shared elements. Because of the reduced dimensions of this combined data set, only hierarchical clustering was used to establish relationships between the three sets of group means (Fig. 8). While relatively coarse-scaled, the comparison shows good agreement for the Kinet local signature, and allows greater concordance between the other compositional subsets of each study.

For KH1 the match between the local Iron Age painted wares of the Hodos et al. study and the large KH1.1 group supports the observation that this group represents a wider local assemblage and the majority of local decorated wares. However, the Blackman and Redford medieval group that included kiln debris, and was therefore assumed to represent local sediments, best matched KH1.3. This group, without a match in the immediate environs of the site, is most closely matched with the southern sediments. Unlike our proposed scenario for the Iron Age where the presence of KH1.3 wares at Kinet indicates import of wares from more coastal areas to the immediate south of the site, the decorated glazed wares targeted in the Blackman and Redford study appear to be the product of a more extended, and sophisticated, system of production in the medieval period, with non-local clays being moved to Kinet. Logistically the import of clays in the medieval period

would appear to flag a deficiency in local resources that is paralleled by the modern import of clays from the same or similar southern sources for tile factories in the area. Coastal shipment of raw materials is also paralleled in the LBA shipment of basalt foundation stones from 25 km north of the site (Fig. 1b).

The likelihood of multiple regional origins for the KH2 class of wares is highlighted in the matches between KH 2.1 and Blackman and Redford's al-Mina local group (B&R 2), between Hodos 1 and Blackman and Redford's ''Cilician'' group (B&R 3), and the inclusion of other ''regional'' groups (Hodos 2 and 3). The likely diversity of the KH2 subsets is further supported by the few KH2 samples that are typologically linked to different places from Cyprus (Fig. 4b 3) to the Levant (Fig. 4b 14). It is apparent that the ''regional'' groups of these two studies are samples of KH2, and that this group represents a widespread (coastal?) sediment type.

The match between KH3A, B&R1, and the more distant Hodos 1.1, supports an origin for these groups in a generically similar geological source. Unfortunately, the coarse scale of this comparison does not allow closer matching with the range of KH3 subsets.

KH4 is a compositionally highly distinctive end member of the PCA projection, where Hodos 3.1/KH2.6 are intermediate between KH4 and KH2 (Fig. 3a). KH4 belongs to a well recognized LBA Cypriot type (white slipped 'milk bowls'). It can be provenanced with some precision through a close match with a NAA fingerprint to a Cypriot volcanic (Troodos)

source. The compositional match between Hodos 3.1 and KH 2.6 shares a pattern of comparatively high scandium concentrations and depleted trace elements. These two groups have the same decoration (black on red banded ware). Because of this compositional and decorative similarity we suggest that the distinctive igneous petrology noted for the Hodos 3.1, indicates a common volcanic origin for both groups. While there is no compositional overlap between KH2.6/Hodos 3.1 and KH4 in the PCA trajectory, they share a comparable pattern of elemental concentrations and a volcanic origin. The compositional offset between these groups may reflect technological/ refinement differences between hand made (KH4) and wheel made wares (KH2.6) and/or different provenances within the same general volcanic precinct in Cyprus.

8. Discussion and conclusions

We are now in a position to discuss the results of the ceramic compositional analysis in terms of political dynamics. NAA has allowed identification of the major compositional groups present in a comparatively large and diverse LBA and IA sample of the excavated assemblage from Kinet Höyük. To differentiate imported and regional wares, a broad based (bottom up) sampling strategy was combined with typological (top down) controls, where available, as a further guide to group identification. To define local production we compared ceramic compositions to sediments collected from around the site and its wider catchment.

Three major compositional groups were broadly identified as non-local, with KH2 typologically linked to a range of production centers in Cyprus, Cilicia (South coastal Turkey) and the Levant, KH3 representing more distant Ionian (coastal Western Turkey), and East Greek centers, and KH4 to the Troodos massif in Cyprus. At a coarse level, the chronological behavior of these groups fits into a two phase pattern of interaction, the first in the MIA, in which KH2 (regional and Cypriot) production centers dominate, and a second in the LIA where (more distant) KH3 centers are most heavily represented. Others have used ceramic typologies of sites to argue for a major post mid 7th century B.C. shift in the pattern of long-distance trade, especially the displacement of Cypriot ceramics by Greek imports (Lehmann, 1998). For Kinet, this suggested shift appears consistent with the pattern of a peak in KH2 classes in the Middle Iron Age and their displacement by KH3 wares in the Late Iron Age. It suggests that for this part of the Eastern Mediterranean the new phase of competition for local markets was largely with products from centers in East Greece and Western Anatolia. The compositional evidence of shifts in local, regional, and exotic production and exchange over time at Kinet suggest rapid transformation in political scale and interaction. The MIA appears to be a critical period for local/regional polity formation.

From the perspective of a small mainland settlement, the displacement of one source of tradewares (Cyprus) with another (Aegean/Greek/Ionian) represents a remotely driven change, beyond the influence of, and with little direct political consequence for local polities. But the evidence for KH2 representing a range of regional centers both in Cyprus and along the mainland coast, suggests this scenario underestimates the local political ramifications of such a shift. If KH2 imports represent sites within this east Mediterranean sphere and KH3 imports indicate long distance interaction with more distant centers, then the intensified regional interaction that commences at the end of the Early Iron Age and peaks in the Middle Iron Age might also be tracking the formation of a local polity at, or near, Kinet. The virtual disappearance of KH2 classes from the Kinet assemblage after the MIA would also not only mark the collapse of a regional production and exchange network but also region-wide political disruption. The expansion of the Neo-Assyrians at this time may well be an important factor in this disruption. The subsequent pattern of trade, where Kinet is without the types of tradewares available at sites better located to exploit East West trade routes, suggests this regional political integration was followed by political marginalization in the LIA.

A major goal of this paper was to establish the scale and extent of local ceramic production at Kinet as a basis for understanding regional political and economic dynamics. Incorporating previous NAA datasets for this site allowed us to better define the range of our regional groups. Our bottom-up sampling strategy combined a wide range of ceramic types with local sediments to identify the most likely compositional signature of local production. Notwithstanding the absence or currency of published standards from which to calculate correction factors, results across the NAA dataset of this study and previously published NAA datasets for Kinet appear directly comparable. The comparison of sediment and ceramic compositions (KH1.1/KH1.2 to Hodos 4; KH1.3 to B&R 4) links these groups to the dominant ophiolitic geology of the coastal range in the vicinity of Kinet. The link between KH1.1 and Hodos 4 and sediments up to 20 km east of Kinet provides the likely scale of the local source, while the disappearance of KH1.2 during the EIA may reflect specific changes in the local production economy as Hittite influence waned. The sediment comparison also shows that the local medieval compositional signature does not match these local sediments but more southerly clay beds. In the medieval period (as for tileworks in the area today), pottery clays, located around Iskenderun appear to have supplied coastal sites like Kinet. It highlights the need for caution when assuming local production equates with local clays, particularly for coastal sites with the ready capacity to ship raw materials.

With a few exceptions, defining the origins of the non-local component of our ceramic sample with any precision was beyond the scope of this paper. However, we suggest that the relative lack of compositional differentiation in KH2 and its apparent wide geographic range will continue to pose significant challenges for future provenance work in this region.

Acknowledgments

References

Adams, R.M., 1981. Heartland of Cities. Chicago University Press, Chicago.

Adams, R.M., Nissen, H.J., 1972. The Uruk Countryside: The Natural Setting of Urban Societies. University of Chicago Press, Chicago.

Baxter, M.J., 1994. Exploratory Multivariate Analysis in archaeology. Edinburgh University Press, Edinburgh.

Baxter, M.J., 2001a. Methodological issues in the study of assemblage diversity. American Antiquity 66 (4), 715—725.

Baxter, M.J., 2001b. Statistical modelling of artefact compositional data. Archaeometry 43 (1), 131—147.

Baxter, M.J., 2006. A review of supervised and unsupervised pattern recognition in archaeometry. Archaeometry 48 (4), 671—694.

Beier, T., Mommsen, H., 1994a. A method for classifying multidimensional data with respect to uncertainties of measurement and Its application to archaeometry. Naturwissenchaften 81, 546—548.

Beier, T., Mommsen, H., 1994b. Modified Mahalanobis filters for grouping pottery by chemical composition. Archaeometry 36 (2), 287—306.

Bishop, R.L., Blackman, M.J., 2002. Instrumental Neutron Activation Analysis of archaeological ceramics: scale and interpretation. Accounts of Chemical Research 35 (8), 603—610.

Blackman, M., Redford, S., 2005. Neutron Activation Analysis of medieval ceramics from Kinet, Turkey, especially Port Symeon ware. Ancient Near Eastern Studies 42, 83—186.

Blackman, M.J., Stein, G.J., Vandiver, P.B., 1993. The standardization hypothesis and ceramic mass production: technological, compositional, and metric indexes of craft specialization at Tell Leilan, Syria. American Antiquity 58 (1), 60—80.

Blanton, R., 2004. Settlement pattern and population change in Mesoamerican and Mediterranean civilizations: a comparative perspective. In: Alcock, S., Cherry, J. (Eds.), Side-by-Side Survey: Comparative Regional Studies in the Mediterranean World. Oxbow Books, Oxford, pp. 206—240.

Boardman, J., 1965. Tarsus, Al Mina and Greek chronology. Journal of Hellenic Studies 85, 5—15.

Brodie, N.J., Steel, L., 1996. Cypriot Black-on-Red: towards a characterisation. Archaeometry 38 (2), 263—278.

Carpenter, R., 1966. Discontinuities in Greek Civilisation. Cambridge University Press, Cambridge.

Clayton, S., 2006. Interregional relationships in Mesoamerica: interpreting Maya ceramics at Teotihuacan. Latin American Antiquity 16 (4), 427—448.

Dibble, H., 1988. Typological Aspects of Reduction and Intensity of Utilization. In: University Museum Symposium Series, Vol. 1. University Museum, University of Pennsylvania, Philadelphia.

Dorais, M.J., Lindblom, M., Shriner, C.M., 2004. Evidence for a single clay/temper source for the manufacture of Middle and Late Helladic Aeginetan pottery from Asine, Greece. Geoarchaeology 19 (7), 657—684.

Ericson, J.E., Glascock, M.D., 2004. Subsource characterization: obsidian utilization of subsources of the Coso volcanic field, Coso Junction, California, USA. Geoarchaeology 19 (8), 779—805.

Glascock, M., 1992. Neutron activation analysis. In: Neff, H., (Ed.), Chemical Characterisation of Ceramic Pastes in Archaeology. Prehistory Press, Madison, WI, pp. 11—26.

Glascock, M.D., 2002. Obsidian provenance research in the Americas. Accounts of Chemical Research 35 (8), 611—617.

Glascock, M.D., Neff, H., 2003. Neutron activation analysis and provenance research in archaeology. Measurement Science and Technology 14, 1516—1526.

Glascock, M.D., Neff, H., Vaughn, K.J., 2004. Instrumental neutron activation analysis and multivariate statistics for pottery provenance. Hyperfine Interactions 154, 95—105.

Gomez, B., Neff, H., Rautman, M.L., Vaughan, S.J., Glascock, M.D., 2002. The source provenance of Bronze Age and Roman pottery from Cyprus. Archaeometry 44 (1), 23—36.

Grave, P., Lisle, L., Maccheroni, M., 2005. Multivariate comparison of ICP-OES and PIXE-PIGE analysis of East Asian storage jars. Journal of Archaeological Science 32 (6), 885—896.

Grave, P., Potts, D.T., Yassi, N., Reade, W., Bailey, G., 1996. Elemental characterisation of Barbar ceramics from Tell Abraq. Arabian Archaeology and Epigraphy 7, 177—187.

Harbottle, G., 1982. Provenience studies using neutron activation analysis: The role of standardisation. In: Olin, J.S., Franklin, A.D. (Eds.), Archaeological Ceramics. Smithsonian Institution Press, Washington, pp. 67—78.

Harbottle, G., 1991. The efficiencies and error-rates of Euclidian and Mahalanobis searches in hypergeometries of archaeological ceramic compositions. In: Pernicka, E., Wagner, G. (Eds.), Archaeometry '90. Birkhauser, Basel, pp. 413—423.

Harbottle, G., Hughes, M.J., Saleem, S., 2005. The origin of black-figure Greek ceramics found in Naucratis. Archaeometry 47 (3), 511—518.

Harrison, T.P., Hancock, R.G.V., 2005. Geochemical analysis and sociocultural complexity: a case study from Early Iron Age Megiddo (Israel). Archaeometry 47 (4), 705—722.

Hein, A., Tsolakidou, A., Iliopoulos, I., Mommsen, H., Buxeda, J., Garrigos, I., Montana, G., Kilikoglou, V., 2002. Standardisation of elemental analytical techniques applied to provenance studies of archaeological ceramics: an inter-laboratory calibration study. Analyst 127, 542—553.

Hodos, T., Knappett, C., Kilikoglou, V., 2005. Middle and Late Iron Age painted ceramics from Kinet Höyük. Anatolian Studies 55, 61—87.

Jones, R.E., 1986. Techniques and methodology in characterisation and provenance work. In: Jones, R. (Ed.), Greek and Cypriot Pottery: A Review of Scientific Studies. The British School at Athens, Athens, pp. 15—56.

King, R.H., Rupp, D.W., Sorenson, L.W., 1986. A multivariate analysis of pottery from southwestern Cyprus using Neutron Activation Analysis data. Journal of Archaeological Science 13, 361—374.

Knappett, C., Kilikoglou, V., Steele, V., Stern, B., 2005. The circulation and consumption of Red Lustrous Wheelmade ware: petrographic, chemical and residue analysis. Anatolian Studies 55, 25—59.

Lehmann, G., 1998. Trends in the local pottery development of the Late Iron Age and Persian Period in Syria and Lebanon, ca. 700 to 300 B.C. Bulletin of the American Schools of Oriental Research 311, 7—37.

Lehmann, G., 2005. Al Mina and the East, a report on research in progress. In: Villing, A. (Ed.), The Greeks in the East. British Museum, London, pp. 61—92.

Liddy, D.J., 1988. A chemical study of Early Iron Age pottery from the North Cemetery. In: Jones, R.H., Catling, H.W. (Eds.), New Aspects of Archaeological Science in Greece. BSA Fitch Lab Occasional Papers, Athens, pp. 29—32. Knossos.

Magee, P., 2004. The impact of southeast Arabian intra-regional trade on settlement location and organization during the Iron Age II period. Arabian Archaeology and Epigraphy 15 (1), 24—42.

Mommsen, H., Kreuser, A., Weber, J., 1988. A method for grouping pottery by chemical composition. Archaeometry 30 (1), 47—57.

Neff, H., 2000. Neutron Activation Analysis for provenance determination in archaeology. In: Ciliberto, E., Spoto, G. (Eds.), Modern Analytical Methods in Art and Archaeology. John Wiley & Sons, New York, pp. 81—134.

Polanyi, K., 1963. Ports of trade in early societies. Journal of Economic History 23 (1), 30—45.

Rhode, D., 1988. Measurement of archaeological diversity and the sample-size effect. American Antiquity 53 (4), 708—716.

SAS Institute, 2006. JMP Statistical Discovery. SAS Institute Inc.

Schwedt, A., Mommsen, H., 2004. Clay paste mixtures identified by Neutron Activation analysis in pottery of a Roman workship in Bonn, Germany. Journal of Archaeological Science 31, 1251—1258.

Sherratt, A., 1993a. What would a Bronze-Age World System look like? Relations between temperate Europe and the Mediterranean in later prehistory. Journal of European Archaeology 1 (2), 1—57.

Sherratt, A., 1993b. 'Who are you calling peripheral?': dependence and independence in European prehistory. In: Scarre, C., Healy, F. (Eds.), Trade and Exchange in Prehistoric Europe. Oxbow Books, University of Bristol, pp. 245—255.

Sherratt, S., Sherratt, A., 1993. The growth of the Mediterranean economy in the early first millennium BC. World Archaeology 24 (3), 361—378.

Summerhayes, G.R., Bird, R., Fullagar, R., Gosden, C., Specht, J., Torrence, R., 1998. Application of PIXE-PIGME to archaeological analysis of changing patterns of obsidian use in West New Britain, Papua New Guinea. In: Shackley, S. (Ed.), Advances in Archaeological Volcanic Glass Studies. Plenum Press, New York, pp. 129—158.

Tykot, R.H., 2002. Chemical fingerprinting and source tracing of obsidian: the central Mediterranean trade in black gold. Accounts of Chemical Research 35 (8), 618—627.

Unruh, J., Johnson, J., 2005. Recent conservation research: soluble salts in Gordion ceramics. In: Kealhofer, L. (Ed.), The Archaeology of Midas and the Phrygians: Recent Work at Gordion. University of Pennsylvania Museum Press, Philadelphia, pp. 204—214.

Wilson, L., Pollard, A.M., 2001. The provenance hypothesis. In: Brothwell, D.R., Pollard, A.M. (Eds.), Handbook of Archaeological Sciences. John Wiley & Sons, Chichester, pp. 507—517.

Woolley, L., 1946. Syria as the gateway between East and West. Geographical Journal 107 (5/6), 179—190.